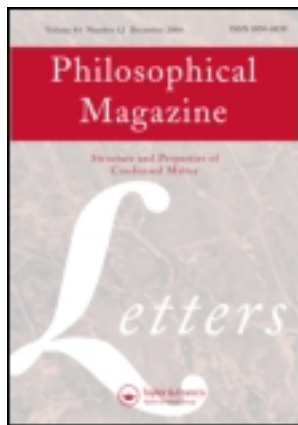


This article was downloaded by: [Pennsylvania State University]

On: 23 December 2011, At: 22:11

Publisher: Taylor & Francis

Informa Ltd Registered in England and Wales Registered Number: 1072954 Registered office: Mortimer House, 37-41 Mortimer Street, London W1T 3JH, UK



Philosophical Magazine Letters

Publication details, including instructions for authors and subscription information:

<http://www.tandfonline.com/loi/tphl20>

Thermodynamic fluctuations in magnetic states: Fe₃Pt as a prototype

Y. Wang^a, S.L. Shang^a, H. Zhang^a, L.-Q. Chen^a & Z.-K. Liu^a

^a Department of Materials Science and Engineering, The Pennsylvania State University, University Park, PA 16802, USA

Available online: 30 Jul 2010

To cite this article: Y. Wang, S.L. Shang, H. Zhang, L.-Q. Chen & Z.-K. Liu (2010): Thermodynamic fluctuations in magnetic states: Fe₃Pt as a prototype, *Philosophical Magazine Letters*, 90:12, 851-859

To link to this article: <http://dx.doi.org/10.1080/09500839.2010.508446>

PLEASE SCROLL DOWN FOR ARTICLE

Full terms and conditions of use: <http://www.tandfonline.com/page/terms-and-conditions>

This article may be used for research, teaching, and private study purposes. Any substantial or systematic reproduction, redistribution, reselling, loan, sub-licensing, systematic supply, or distribution in any form to anyone is expressly forbidden.

The publisher does not give any warranty express or implied or make any representation that the contents will be complete or accurate or up to date. The accuracy of any instructions, formulae, and drug doses should be independently verified with primary sources. The publisher shall not be liable for any loss, actions, claims, proceedings, demand, or costs or damages whatsoever or howsoever caused arising directly or indirectly in connection with or arising out of the use of this material.

Thermodynamic fluctuations in magnetic states: Fe₃Pt as a prototype

Y. Wang*, S.L. Shang, H. Zhang, L.-Q. Chen and Z.-K. Liu

*Department of Materials Science and Engineering, The Pennsylvania
State University, University Park, PA 16802, USA*

(Received 10 May 2010; final version received 12 July 2010)

To understand the Invar anomalies, such as negative thermal expansion and spontaneous magnetization, we have applied our recently developed thermodynamic framework for a system with itinerant-electron magnetism to the ordered Fe₃Pt. The framework has coherently predicted the finite temperature intermixing between the fully ferromagnetic (FM) configuration and the spin-flipping configurations (SFCs). We have also discovered a tri-critical point at which a high-temperature second-order phase transition, between the fully ordered FM phase and the paramagnetic phase which is disordered due to SFCs, becomes first order at low temperatures.

Keywords: magnetic phase transition; thermal expansion; first-principles calculations; Invar

Invar was discovered in intermetallic Fe₆₅Ni₃₅ alloy in 1897 by Guillaume [1] who received a Nobel Prize in Physics in 1920 for the discovery. It is characterized by “anomalies”, including thermal expansion, equation-of-state, elastic modulus, heat capacity, magnetization, and Curie temperature, etc [2]. However, despite extensive theoretical and experimental activities [2–20] over the last century, stimulated by their wide-spread applications in scientific instruments, there is a lack of a microscopic understanding that can satisfactorily explain all the Invar anomalies. The primary existing theoretical models for Invar include: (1) the Weiss 2- γ model [6,10,15]; (2) the non-collinear spin model [11,16]; and (3) the disordered local moment (DLM) approach [18,21]. The 2- γ model relies on the existence of two distinct magnetic states for Fe: a high-spin state and a low-spin state, the latter having a lower volume and a slightly higher energy of ~ 1 mRy [12]. In this model, the anomalous thermal expansion of Invar is explained by the compensating effects of usual lattice thermal expansion and the thermal excitation between the high-spin and low-spin states. However, the phase transition from the high-spin state to the low-spin state in the 2- γ model is first order while experimental measurements at room temperature (e.g. equation-of-state, see van Schilfhaarde et al. [16]) show a second-order phase transition. Moreover, the state-of-the-art first principles calculations [11,21] indicate that the energy difference between the two states is an

*Corresponding author. Email: yuw3@psu.edu

order of magnitude larger than the value of 1 mRy required by the 2- γ model. The non-collinear spin model interprets the Invar behavior through the continuous variations of the Fe spin alignment and amplitude. It therefore predicts that there should be no first-order discontinuity in the equation-of-state at any temperature. However, very recent measurements of pressure vs. volume curves at 30 K by Nataf et al. [22] clearly shows a first-order transition of Fe₇₂Pt₂₈ at 5.7 GPa and a “bump” (at least a change of the curvature sign) presented for Fe₆₄Ni₃₆ between 2.5 and 4.5 GPa. In addition, recent neutron scattering experiments by Wildes and Cowlam [20] did not find the non-collinear state. The work by Uhl et al. [11], which was based on the non-collinear model and was quoted by Shiga [13] as the best theoretical study so far published on Fe₃Pt, can only predict thermal expansion with an order of magnitude accuracy. The DLM approaches [18,21] have the ability to account for the possibility of random antiparallel spin alignments, suggesting the importance of multiple magnetic states.

We have been trying to develop a first-principles finite temperature thermodynamic framework [23,24] for a system with itinerant magnetism. This study is inspired by the idea of the DLM approaches [18,21], and in particular, the considerations of the partial disordered local moment (PDLM) by the previous works [21,25,26], aimed to extend the essentially $T=0$ DLM scheme to finite temperatures. We show the application of our framework to the ordered L1₂ Fe₃Pt to study the Invar anomaly at finite temperatures.

In addition to the fully ferromagnetic configuration (FMC) where all the spins on each Fe atom line up along one direction, our framework considers many other spin-flipping configurations (SFCs) with a fraction of the spins in the opposite direction. Above 0 K, each spin configuration has its own characteristic thermal vibration and thermal electronic excitation. We propose that FMC and various SFCs coexist and their thermal populations, dictated by their individual Helmholtz energy levels, are both temperature and volume dependent. We emphasize that our formulism is fundamentally different from the existed models. We first calculate the free energies of each spin configuration as a function of temperature and volume independently and then mix representative spin configurations through statistical analysis at finite temperatures.

We first summarize our theoretical framework [23,24]. Let us consider a lattice with N atoms under the constant volume V and temperature T . We start from the partition function of a specific spin configuration σ , which is known as [27]:

$$Z^\sigma = \sum_{i \in \sigma, \rho \in \sigma} \exp[-\beta \varepsilon_i(N, V, \rho)] = \exp[-\beta F^\sigma(N, V, T)], \quad (1)$$

where $\beta=1/k_B T$, i identifies all the vibrational states within σ , ρ labels the electronic distributions within σ , $\varepsilon_i(N, V, \rho)$ is the eigenvalue of the corresponding microscopic Hamiltonian associated with σ , and $F^\sigma(N, V, T)$ its Helmholtz energy. Then the partition function for a system with multi-spin configurations, Z , can be written as:

$$Z = \sum_{\sigma} w^\sigma Z^\sigma, \quad (2)$$

where w^σ is the multiplicity of the spin configuration σ . It is immediately apparent that $x^\sigma = w^\sigma Z^\sigma / Z$ is the thermal population of the spin configuration σ . Furthermore, with $F = -k_B T \ln Z$ [28], we obtain the Helmholtz energy of the system as:

$$\begin{aligned} F(N, V, T) &= -k_B T \sum_{\sigma} x^\sigma \ln Z^\sigma + k_B T \left[\sum_{\sigma} x^\sigma \ln Z^\sigma - x^\sigma \ln Z \right] \\ &= \sum_{\sigma} x^\sigma F^\sigma(N, V, T) + k_B T \sum_{\sigma} x^\sigma \ln \left(\frac{x^\sigma}{w^\sigma} \right). \end{aligned} \quad (3)$$

Equation (3) relates the total Helmholtz energy of a system with many spin configurations, $F(N, V, T)$, and the Helmholtz energies of individual spin configurations, $F^\sigma(N, V, T)$. An important result of Equation (3) is the configurational entropy of multi-spin configurations.

$$S_f(N, V, T) = -k_B \sum_{\sigma} w^\sigma \left[\left(\frac{x^\sigma}{w^\sigma} \right) \ln \left(\frac{x^\sigma}{w^\sigma} \right) \right]. \quad (4)$$

We use the SFCs derived from a system with 12-atom $3 \times 1 \times 1$ supercell using the ATAT package [29]. Containing nine magnetic atoms, such a system leads to $2^9 = 512$ spin configurations which are, by symmetry, reduced to 37 non-equivalent ones. The ATAT code has been modified to calculate the multiplicities (w^σ) by counting the number of equivalent spin up and down arrangements for each of the 37 spin configuration. One issue to consider is that a 12-atom supercell is not large enough. In statistical modeling, this might give rise to finite size effects which could result in considerable smearing of the order parameter and related quantities in the region of the phase transformation. However, at least for the prototype of $L1_2$ Fe_3Pt used in this study, the 12-atom supercell is sufficiently large to demonstrate the major philosophy of Equation (3). The specific effects of the small system size will be briefly discussed later in this letter as they are associated with the calculated results of thermal expansion and spontaneous magnetization.

We consider contributions to F^σ from three resources: (1) 0 K electronic energy; (2) the lattice vibration; and (3) thermal electronic excitation. To calculate the 0 K energy, we have employed the VASP package within the projector-augmented wave (PAW) method [30,31]. The exchange-correlation part of the density functional is treated within the GGA of Perdew–Burke–Ernzerhof (PBE) with the interpolation formula of Perdew et al. [32]. For all SFCs, the local structures are relaxed. For the evaluation of the thermal electronic excitation, we have employed integration over the electronic density-of-states through Fermi–Dirac distribution adopted in the previous work [33]. For the lattice vibration, we find that the Debye–Grüneisen approach [34,35] is a fast and yet accurate enough solution.

Figure 1 presents the first-principles 0 K total energies of 36 non-equivalent SFCs as well as the FMC as a function of atomic volume. We indeed find a number of SFCs, whose energies are in the range of ~ 1 mRy/atom to that of the FMC. It is interesting to note that all the SFCs studied herein have the equilibrium averaged atomic volumes at least 1.8% smaller than that of the FMC, the 0 GPa ground state.

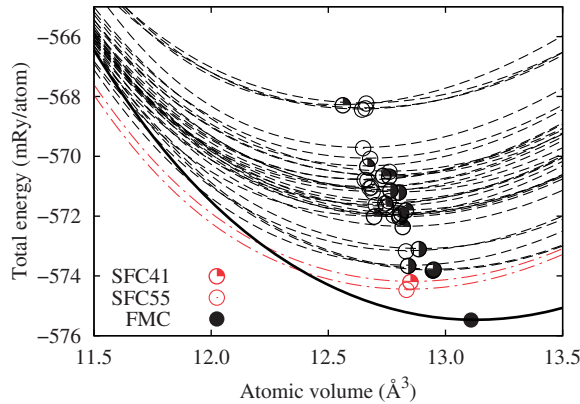


Figure 1. Total energies at 0 K. The heavy black line represents the FMC. The symbols \circ , \odot , \ominus , and \bullet with dashed lines indicate the minima of the energy–volume curves of the SFCs with spin polarization rates of 1/9, 3/9, 5/9, and 7/9, respectively. The red \circ and \odot with dot-dashed lines mark the two lowest SFCs in energy.

In Figure 1, the two lowest energy SFCs have been labeled as SFC55 and SFC41. Their spin arrangements are very similar to the double layer antiferromagnetic state defined by Abrikosov et al. [21]. The calculations done in this study show that the nonmagnetic configuration (not shown in Figure 1) has a very small atomic volume of $11.66 \text{ \AA}^3/\text{atom}$, and its energy is higher than both FMC and all SFCs.

Based on the free energy dependency on temperature and volume, we have calculated the T – V phase diagram that is plotted in Figure 2a. It clearly shows a tri-critical point at $T = 141 \text{ K}$ and $V = 12.61 \text{ \AA}^3$ with $P = 5.81 \text{ GPa}$. Below the tri-critical point, it is a two-phase miscibility gap (the shadow area enclosed by the dotted lines). Above the tri-critical point, the phase transitions between the FM phase at large volumes and the PM phase at small volumes are of second order, for which one cannot define a sole criterion for determining the phase transition. In this study, the transition volumes are determined by the condition that F_{PM} , the free energy counting all SFCs, equals to F_{FM} , the free energy counting only FMC. The existence of such a tri-critical point is supported by experimental measurements [19,22,36]. For example, Abd-Elmeguid and Micklitz [36] observed a critical point at $\sim 110 \text{ K}$ and 6.0 GPa , similar to the values of $\sim 130 \text{ K}$ and 7.0 GPa obtained by Matsushita et al. [19]. We also provide the T – P phase diagram (Figure 2b) showing the phase boundary between FM and PM phases, where the data points are the measured pressure dependence of the Curie temperature (T_c) [19,36]. The agreement between the measurements and our predictions is remarkable. We want to add that the configuration mixing considered in our model through Equation (3) plays key role in predicting the existence of the tri-critical point. For demonstration, we have also calculated phase boundary between FM and PM phases without considering the configuration mixing between the two phases. It is seen that the phase transition between FM and PM phases is always of first order. It should be pointed out that, the classical Weiss 2- γ model [6] predicts only first-order phase transitions while the non-collinear spin model yields only second-order phase transitions at all temperatures [16] as pointed out by Nataf et al. [22].

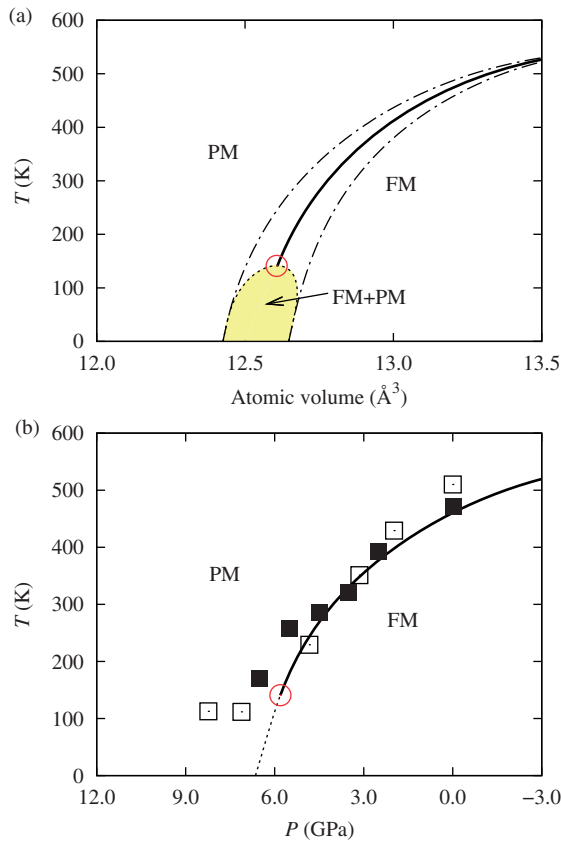


Figure 2. (a) T - V phase diagram of the ordered Fe_3Pt . Yellow shadow, the predicted region of two phase mixture; Solid line, the calculated tentative phase boundary above the tri-critical point (\circ). The dot-dashed lines denote the calculated phase boundary without considering the configuration mixing between ferromagnetic (FM) phase and paramagnetic (PM) phase. (b) T - P phase diagram. Dotted line, the calculated phase boundary (assuming no configuration mixing) below the tri-critical temperature; \square , Curie temperature (T_c) of $\text{Fe}_{72}\text{Pt}_{28}$, measured by Abd-Elmeguid and Micklitz [36], and \blacksquare , T_c of $\text{Fe}_{72.8}\text{Pt}_{27.2}$, measured by Matsushita et al. [19].

We illustrate the predicted thermal volume expansion in Figure 3a and the derived linear thermal expansion (LTE) coefficient in Figure 3b. No experimental data appears to be available in the literature for the fully ordered phase. For comparison, we therefore include the available experimental data for Fe_3Pt measured by Sumiyama et al. [8] (indicated with a parameter called as order parameter $S=0.92$), $\text{Fe}_{72}\text{Pt}_{28}$ measured by Sumiyama et al. [7] ($S=0.86$), and $\text{Fe}_{72}\text{Pt}_{28}$, shown by Rellinghaus et al. [12] ($S \geq 0.90$). We predicted a positive thermal expansion from 100 to 288 K, followed by a negative thermal expansion in the range of 289–449 K, and then a positive thermal expansion again at >450 K, in excellent agreement with experiments [7,8,12]. The only disagreement between our calculations and experiments occur at $T < 100$ K where the calculations did not reproduce the negative

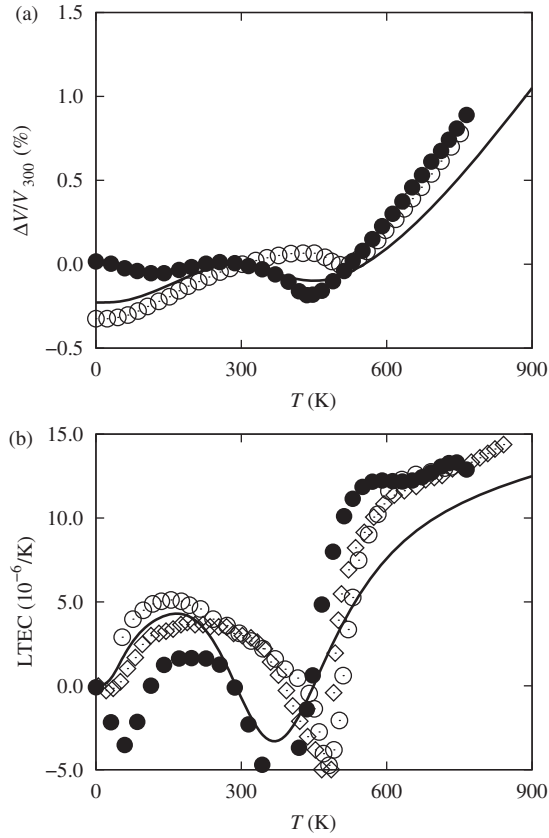


Figure 3. (a) Relative volume increase $(V - V_{300})/V_{300}$ with V_{300} being the equilibrium volume at 300 K and 0 GPa for the ordered Fe₃Pt. (b) LTE coefficient. Solid line, the calculations done in this study; ○, Fe₇₂Pt₂₈, measured by Sumiyama et al. [7] (with order parameter $S = 0.86$); ●, Fe₃Pt measured by Sumiyama et al. [8] ($S = 0.92$) and ◇, Fe₇₂Pt₂₈ shown by Rellinghaus et al. [12] ($S \geq 0.90$).

thermal expansion for Fe₃Pt. Large supercells may be necessary for low temperatures.

To fully understand Invar, an attempt is made to develop a formulation to calculate its spontaneous magnetization, $M_s(T)$. The formulation of $M_s(T)$ of Invar has been enduring challenges as both the Bloch $T^{3/2}$ and the Stoner T^2 laws [28] failed to describe the magnetic moment dependence on temperature of Invar. Wasserman [2], Maruyama [37], Maruyama et al. [38] and Shen et al. [39] proposed a fitting formula by combing the spin-wave excitations and a second excitation whose physical nature was unknown.

We postulate that $M_s(T)$ of Invar is a thermal average over the spontaneous magnetization of the individual spin configuration as:

$$M_s(T) = \sum_{\sigma} x^{\sigma} M_s^{\sigma}(T), \quad (5)$$

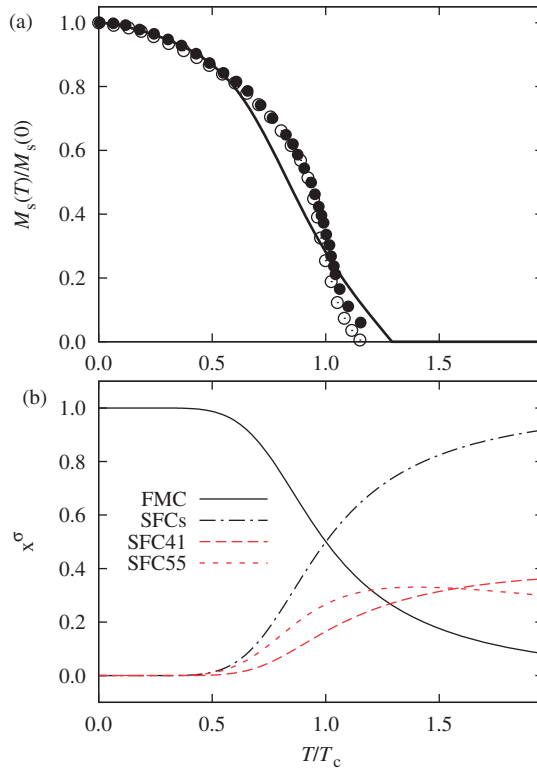


Figure 4. (a) Reduced spontaneous magnetization, $M_s(T)/M_s(0)$, vs. reduced temperature, T/T_c . Solid line, the calculations done in this study; \circ , $\text{Fe}_{72}\text{Pt}_{28}$ from the review work by Wasserman [2]; \bullet , $\text{Fe}_{70}\text{Pt}_{30}$ measured by Shen et al. [39]. (b) The calculated thermal populations of the FMC (black solid line) and that of the sum over all SFCs (black dot-dashed line). The two major contributions to the PM phase are from SFC55 and SFC41, which are plotted using red dashed and long dashed lines, respectively.

with that the spontaneous magnetization of the FMC, $M_{\text{SW}}^{\text{FMC}}(T)$, obeys the spin-wave theory with the Bloch $T^{3/2}$ form [28] and the spontaneous magnetization of the SFC, $M_{\text{MF}}^{\text{SFC}}(T)$, obeys the mean-field theory with the Brillouin expression [28].

The calculated spontaneous magnetization and thermal populations of FMC and that of the sum over all SFCs vs. temperature curves are plotted in Figure 4a and b. It can be seen that the two major contributions to the PM phase are from SFC55 and SFC41. Our calculated $M_s(T)$ demonstrates several important physics for Invar:

- (1) At low temperature ($T/T_c < 0.5$), $M_s(T)$ is completely dictated by the FMC (Figure 4a), as it is seen that x^{FMC} takes its maximum value of 1.0 for $T/T_c < 0.5$ (Figure 4b).
- (2) For $T/T_c > 0.5$, Figure 4b shows that x^{FMC} decreases in an exponential form which results in a “tail” on $M_s(T)$ around $T_c = 460$ K (Figure 4a), in agreement with the experiments [2,39].

Lastly, two effects can be attributed to the use of small 12-atom supercell: the tail in the calculated magnetization curves shown in Figure 4a; and the deviation of the calculated LTE, in particular, the calculated broadening of the LTE around the transition temperature, shown in Figure 3 from the rather sharp experimental anomaly observed by Rellinghaus et al. [12]. However, substantially larger system sizes would boost the computational demands and make this study unfeasible. The focus of this article is on the physics of incorporating finite temperature into the formulation of Helmholtz free energy through Equation (3) and many basic Invar related properties are reproduced very well, as indicated in this article.

In summary, through explicitly considering the freedom of spin in partition function, we have developed a first principles formulation of the Helmholtz energy for materials that exhibit thermodynamic fluctuations among different spin configurations. Illustrated with Fe_3Pt , the observed Invar anomalies are successfully described within this framework.

Acknowledgements

We thank Mr. J.E. Saal for facilitating valuable discussions. This study was funded by the Office of Naval Research (ONR) under Contract No. N0014-07-1-0638, the National Science Foundation (NSF) through Grant No. DMR-0510180, and DOE Basic Sciences under Grant No. DOE DE-FG02-07ER46417 (Yi Wang and Chen), and in part supported by instrumentation funded by the National Science Foundation through grant OCI-0821527. Calculations were also conducted at the LION clusters at the Pennsylvania State University and at the National Energy Research Scientific Computing Center, which is supported by the Office of Science of the US Department of Energy under Contract No. DE-AC02-05CH11231. This study was also supported in part by a grant of HPC resources from the Arctic Region Supercomputing Center at the University of Alaska Fairbanks as part of the Department of Defense High Performance Computing Modernization Program.

References

- [1] C.E. Guillaume, C.R. Acad. Sci. 125 (1897) p.235.
- [2] E.F. Wasserman, *Invar: moment-volume instabilities in transition metals and alloys*, in *Handbook of Ferromagnetic*, Chap. 3, Vol. 5, K.H.J. Bushow and E.P. Wohlfarth, eds., Elsevier Science Publishers B.V., Amsterdam, 1990, p.237.
- [3] K. Honda, Nature 131 (1933) p.587.
- [4] L.F. Bates and J.C. Weston, Nature 145 (1940) p.550.
- [5] N. Ananthanarayanan and R.J. Peavler, Nature 192 (1961) p.962.
- [6] R.J. Weiss, Proc. R. Soc. Lond. A 82 (1963) p.281.
- [7] K. Sumiyama, M. Shiga, M. Morioka and Y. Nakamura, J. Phys. F Met. Phys. 9 (1979) p.1665.
- [8] K. Sumiyama, Y. Emoto, M. Shiga and Y. Nakamura, J. Phys. Soc. Jpn. 50 (1981) p.3296.
- [9] M.M. Abdelmeguid and H. Micklitz, Phys. Rev. B Condens. Matter 40 (1989) p.7395.
- [10] V.L. Moruzzi, Solid State Commun. 83 (1992) p.739.
- [11] M. Uhl, L.M. Sandratskii and J. Kubler, Phys. Rev. B Condens. Matter 50 (1994) p.291.
- [12] B. Rellinghaus, J. Kastner, T. Schneider, E.F. Wassermann and P. Mohn, Phys. Rev. B Condens. Matter 51 (1995) p.2983.
- [13] M. Shiga, Curr. Opin. Solid State Mater. Sci. 1 (1996) p.340.

- [14] M. Uhl and J. Kubler, *J. Phys. Condens. Matter* 9 (1997) p.7885.
- [15] M.E. Gruner, R. Meyer and P. Entel, *Eur. Phys. J. B Condens. Matter* 2 (1998) p.107.
- [16] M. van Schilfgaarde, I.A. Abrikosov and B. Johansson, *Nature* 400 (1999) p.46.
- [17] T. Kakeshita, T. Takeuchi, T. Fukuda, M. Tsujiguchi, T. Saburi, R. Oshima and S. Muto, *Appl. Phys. Lett.* 77 (2000) p.1502.
- [18] S. Khmelevskiy, I. Turek and P. Mohn, *Phys. Rev. Lett.* 91 (2003) p.037201.
- [19] M. Matsushita, S. Endo, K. Miura and F. Ono, *J. Magn. Magn. Mater.* 269 (2004) p.393.
- [20] A.R. Wildes and N. Cowlam, *J. Magn. Magn. Mater.* 272–276 (2004) p.536.
- [21] I.A. Abrikosov, A.E. Kissavos, F. Liot, B. Alling, S.I. Simak, O. Peil and A.V. Ruban, *Phys. Rev. B Condens. Matter* 76 (2007) p.014434.
- [22] L. Nataf, F. Decremps, M. Gauthier and B. Canny, *Phys. Rev. B Condens. Matter* 74 (2006) p.184422.
- [23] Y. Wang, L.G. Hector, H. Zhang, S.L. Shang, L.Q. Chen and Z.K. Liu, *Phys. Rev. B Condens. Matter* 78 (2008) p.104113.
- [24] Y. Wang, L.G. Hector, H. Zhang, S.L. Shang, L.Q. Chen and Z.K. Liu, *J. Phys. Condens. Matter* 21 (2009) p.326003.
- [25] H. Akai and P.H. Dederichs, *Phys. Rev. B Condens. Matter* 47 (1993) p.8739.
- [26] B.L. Györfy, A.J. Pindor, J. Staunton, G.M. Stocks and H. Winter, *J. Phys. F Met. Phys.* 15 (1985) p.1337.
- [27] L.D. Landau and E.M. Lifshitz, *Statistical Physics*, Pergamon Press Ltd., Oxford, New York, 1980–1981.
- [28] C. Kittel, *Introduction to Solid State Physics*, Wiley, Hoboken, NJ, 2005, p.xix.
- [29] A. van de Walle, M. Asta and G. Ceder, *CALPHAD* 26 (2002) p.539.
- [30] P.E. Blöchl, *Phys. Rev. B Condens. Matter* 50 (1994) p.17953.
- [31] G. Kresse and D. Joubert, *Phys. Rev. B Condens. Matter* 59 (1999) p.1758.
- [32] J.P. Perdew, K. Burke and M. Ernzerhof, *Phys. Rev. Lett.* 77 (1996) p.3865.
- [33] Y. Wang and Y.F. Sun, *J. Phys. Condens. Matter* 12 (2000) p.L311.
- [34] V.L. Moruzzi, J.F. Janak and K. Schwarz, *Phys. Rev. B Condens. Matter* 37 (1988) p.790.
- [35] Y. Wang, R. Ahuja and B. Johansson, *Int. J. Quantum Chem.* 96 (2004) p.501.
- [36] M.M. Abd-Elmeguid and H. Micklitz, *Phys. Rev. B Condens. Matter* 40 (1989) p.7395.
- [37] H. Maruyama, *J. Phys. Soc. Jpn.* 55 (1986) p.2834.
- [38] H. Maruyama, R. Pauthenet, J.C. Picoche and O. Yamada, *J. Phys. Soc. Jpn.* 55 (1986) p.3218.
- [39] Y. Shen, Q. Chen, H. Maruyama, I. Nakai and O. Yamada, *J. Magn. Magn. Mater.* 54–57 (1986) p.1083.